Environmental Science & Technology

Article

pubs.acs.org/est

UV Irradiation Induced Transformation of TiO_2 Nanoparticles in Water: Aggregation and Photoreactivity

Jing Sun,[†,‡] Liang-Hong Guo,*[,†] Hui Zhang,*[,†] and Lixia Zhao[†]

[†]State Key Laboratory of Environmental Chemistry and Eco-toxicology, Research Centre for Eco-environmental Sciences, Chinese Academy of Sciences, 18 Shuangqing Road, P.O. Box 2871, Beijing 100085, China

[‡]School of Light Chemistry and Environmental Engineering, Qilu University of Technology, Jinan 250353, China

Supporting Information

ABSTRACT: Transformation of nanomaterials in aqueous environment has significant impact on their behavior in engineered application and natural system. In this paper, UV irradiation induced transformation of TiO_2 nanoparticles in aqueous solutions was demonstrated, and its effect on the aggregation and photocatalytic reactivity of TiO_2 was investigated. UV irradiation of a TiO_2 nanoparticle suspension accelerated nanoparticle aggregation that was dependent on the irradiation duration. The aggregation rate increased from <0.001 nm/s before irradiation to 0.027 nm/s after 50 h irradiation, resulting in aggregates with a hydrodynamic diameter of 623 nm. The isoelectric point of the suspension was lowered from 7.0 to 6.4 after irradiation, indicating less positive charges on the surface. ATR-FTIR spectra displayed successive growth of surface hydroxyl groups with UV irradiation which might be responsible for the change of surface charge and aggregation rate. UV irradiation also changed the photocatalytic degradation rate of Rhodamine B by TiO_2, which initially increased with irradiation time, then decreased. Based on the photoluminescence decay and photocurrent collection data, the change was attributed to the variation in interparticle charge transfer kinetics. These results highlight the importance of light irradiation on the transformation and reactivity of TiO_2 nanomaterials.

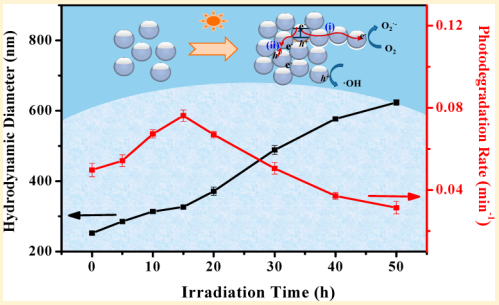

INTRODUCTION

Semiconductor nanomaterials have attracted intensive interest due to their ability to drive photochemical reactions under solar light irradiation.[1−4] In particular, TiO_2 nanoparticles are widely used in photocatalytic devices to achieve environmental remediation and water splitting because of their low-cost, low toxicity and robust performance.[5,6] Modeling studies predicted the annual production of nano-TiO_2 would exceed 2.5 million tons by 2025.[7] With the high reactivity and the rising demand of nano-TiO_2, it is essential to elucidate both their stability in the practical devices during the life cycle of these products and their transformation process after discharge into the natural environment.

Typical transformation processes of nanomaterials include aggregation, dissolution, redox reaction, photochemical reaction, and biocatalyzed degradation.[8−10] A nanomaterial may participate in one or more processes, depending not only on its inherent properties but also on the surrounding environmental factors. Indeed, once introduced to the practical applications, nano-TiO_2 encounters the environmental factors (e.g., natural organic matter, ionic species and sunlight) and then nano-TiO_2 will inevitably undergo physical and chemical transformations due to their high surface reactivity and large specific surface area. These transformation pathways will in turn govern their photoreactivity and environmental fate. Because of its high chemical stability, studies on the nano-TiO_2 behavior are mainly related to aggregation process.[11−13] Typically, The hydroxyl groups covered on nano-TiO_2 surface would interact with different components in natural waters and then cause aggregation occurrence. Nano-TiO_2 aggregation behavior in electrolyte or humic acid solutions has been quantitatively described by the classical Derjaguin−Landau−Verwey−Overbeek (DLVO) theory.[14,15] Wiesner et al. reported that nano-TiO_2 aggregation induced by inorganic ions (or organics) decreased the photoreactivity and reduced reactive oxygen species generation in a fashion dependent on aggregate size and structure.[16] Recently, it was reported that preadsorbed water on nano-TiO_2 surface significantly modulated its surface hydroxyls.[17] This process may also alter its surface chemistry and consequently cause the changes in stability and photoreactivity. Thus, an in-depth understanding of the effect of the exposure environment on nano-TiO_2 transformation is essential in assessing their phtoreactivity and environmental behavior.

As a photoactive nanomaterial, photochemical transformation of nano-TiO_2 is expected to be an important process in aquatic environment. Fujishima et al. reported the amphiphilic-to-hydrophobic conversion on TiO_2 single-crystal surface due to the changes of the adsorbed hydroxyl groups during UV irradiation.[18,19] However, this is a reversible process during the

Received: May 13, 2014
Revised: August 18, 2014
Accepted: September 26, 2014
Published: September 26, 2014

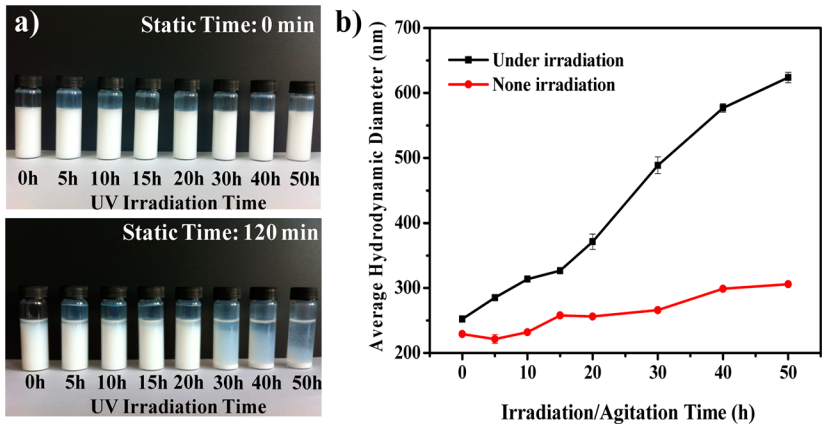

Figure 1. (a) Digital photographs of TiO_2 nanoparticle suspensions (0.25g L^{-1}) taken immediately after UV-irradiation (top), and taken after UV-irradiation and then under static state for 120 min (bottom). (b) Change of the average aggregate size of nano-TiO_2 suspension with UV irradiation time.

UV light "on−off" cycles. The effect of long-term UV irradiation on the transformation of nano-TiO_2 has not been addressed in the literature. Indeed, concerns about the photochemical behaviors of nano-TiO_2 have stimulated two important issues. One is the photoreactivity of nano-TiO_2 after prolonged use under light irradiation. This would determine the lifetime of this material in engineered applications. Another issue is the possible photochemical transformation after long-term sunlight irradiation, which would determine its environmental fate, transport and toxicity.

In the present study, we investigated the aggregation behavior of P25 TiO_2 nanoparticles after UV irradiation, and identified TiO_2 surface hydroxyl groups as the source for the change of its aggregation kinetics. The effect of the size and structure of the TiO_2 aggregates on its photocatalytic properties were also evaluated. The results are significant for interpreting the TiO_2 behavior in engineered applications as well as in natural system where nanoparticles may aggregate after long-term irradiation.

EXPERIMENTAL SECTION

Chemicals. TiO_2 nanoparticles (Aeroxide P25, 80% anatase and 20% rutile, primary particle size: ~21 nm) and terephthalic acid were purchased from Sigma-Aldrich (St. Louis, MO). Methyl viologen was obtained from J&K Chemical Ltd. (Shanghai, China). Rhodamine B (RhB) was purchased from Sinopharm Chemicals Corporation (Shanghai, China). All other chemicals were of analytical reagent grade and used as received without further purification. Deionized water (resistance >18 MΩ cm) was prepared on a Millipore Milli-Q system (Bedford, MA) and used throughout all experiments.

UV Irradiation Experiments. A TiO_2 suspension was prepared by adding 0.75 g TiO_2 powder to 300 mL deionized water and then sonicated and stirred for 1 h, respectively. The ultrasound irradiation was performed in an ultrasonic cleaner (KQ250-DB, Kunshan Ultrasound Instrument Co., China) with a frequency of 40 kHz and an ultrasound input power of 250 W. The above TiO_2 suspension was transferred into a cylindrical Pyrex glass reactor and then illuminated by UV light provided by a 500 W tube-like high pressure mercury lamp (Perfectlight Co., Beijing, China) with a irradiation intensity of 5 mW cm^{-2} and maximum emission at approximately 365 nm. The TiO_2 suspension was irradiated for up to 50 h under stirred state. An aliquot of the suspension was taken out every 5 or 10 h during the irradiation for characterization. The control sample of TiO_2 suspension without irradiation was prepared by a similar protocol and agitated in the dark for up to 50 h. All the experiments were carried out under ambient conditions and the temperature was maintained at 20 °C.

Characterization. Nanoparticle aggregate size was determined by dynamic light scattering (DLS) analysis (Malvern Zetasizer Nano ZS, Malvern Instruments, Worcestershire, UK). All the DLS measurements were performed with the same time delay (10 min) to reduce experiment errors. The hydrodynamic diameter is the average of three measurements, each consisting of six consecutive runs. Zeta potentials and the electrophoretic mobility (EPM) of the particles were measured with a zetasizer Nano ZS (Malvern Instruments, Worcestershire, UK). For zeta potential measurements, the pH was adjusted with NaOH or HCl solution. Each sample was measured three times, each consisting of 12 runs, using folded capillary cells. All size and zeta potentials measurements were conducted at 25 °C. Particle morphology was examined using a transmission electron microscopy (TEM, HITACHI H-7500, Japan). ATR-FTIR measurements were performed using a Thermo-Nicolet Nexus 6700 FTIR spectrometer equipped with an ATR Max II horizontal flow cell (PIKE Technologies, Madison, WI) and a liquid nitrogen-cooled mercury−cadmium−telluride (MCT) detector. The above TiO_2 suspension was added onto a ZnSe crystal. The spectra were recorded using 128 scans at 2 cm^{-1} resolution. Crystal structure was measured by the powder X-ray diffraction (XRD) using X'Pert PRO MPD (Philips, Eindhoven, Netherlands) with Cu Kα radiation. Raman spectroscopy measurements were performed on Renishaw inVia Raman spectrometer (Wotton-under-Edge, UK) with exciting wavelength at 532 nm. Photoluminescence lifetime decay of irradiated TiO_2 sample was recorded on an Edinburgh Instruments F900 spectrometer (Livingston, UK) with a 375 nm laser excitation source and luminescence monitored at 430 nm. All the irradiated TiO_2 samples were kept stirring until the measurements were conducted.

Photoreactivity Performance. Photoreactivity of TiO_2 samples was evaluated by the photodegradation of RhB. An aliquot of TiO_2 stock suspension with different irradiation time was taken out and then RhB stock solution was added. The above solution was diluted to 100 mL with a final TiO_2 concentration of 250 mg L^{-1} and RhB concentration of 10 mg L^{-1}. The resulting suspension was stirred for 30 min in the

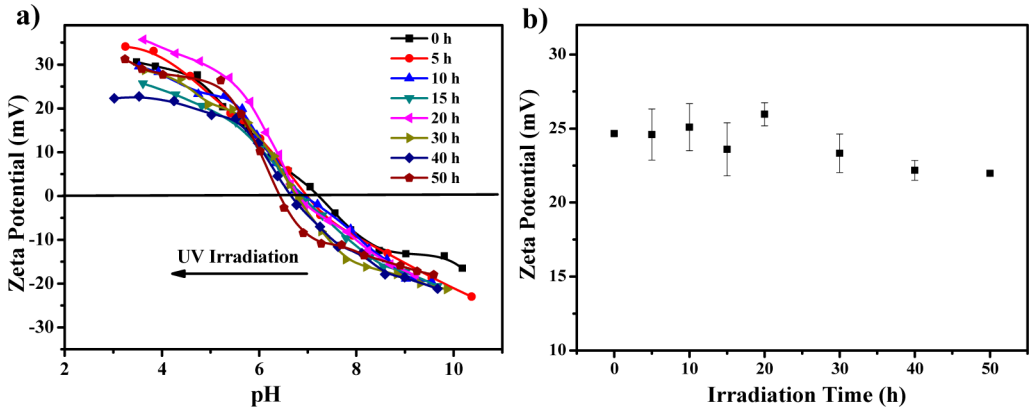

Figure 2. (a) Variation of the zeta potential of the irradiated TiO_2 suspension (0.25 g L^{-1}, 20 °C) as a function of pH, and (b) Variation of the zeta potential of TiO_2 suspension with different UV irradiation time measured at native solution pH of 5.40.

dark to ensure adsorption/desorption equilibrium. Then the above suspension was transferred into the cylindrical Pyrex glass reactor and illuminated with the 500 W tube-like high pressure mercury lamp. At a given time interval of irradiation, 2 mL aliquots were collected from the suspension and centrifuged. The residual concentration of RhB in the aliquot was analyzed by using an Agilent 8453 UV−vis spectrophotometer (Palo Alto, CA) at a wavelength of 553 nm.

Hydroxyl radicals were quantified by the terephthalic acid (TA) fluorescence assay.[20] A mixed suspension containing the irradiated TiO_2 sample (1 mg L^{-1}, 50 mL) and TA (3 mM, 2 mL) was irradiated with a 500 W Xe arc lamp (Beijing Trust-Tech Company, China) with a cutoff filter (λ < 400 nm). Fluorescence emission intensity of the product, 2-hydroxyterephthalic acid (TAOH) was measured on a Horiba Fluoromax-4 spectrofluorimeter (Edison, NJ) with excitation wavelength at 312 nm and emission wavelength at 426 nm. All the photocatalytic experiments were performed in triplicates and the mean values are reported.

Photoelectrochemical Measurement. Photocurrent collection from the illuminated TiO_2 suspension was carried out in a three-electrode cell with a Pt plate working electrode (10 mm length × 8 mm width), a graphite rod counter electrode, and an Ag/AgCl reference electrode.[21] A TiO_2 suspension was magnetically stirred under N_2 gas saturation during the UV irradiation with methyl viologen (1 mM), KNO_3 (5 mM) and CH_3OH (10% v/v) as the electron shuttle, electrolyte and hole scavenger, respectively. Photocurrent was measured on a CHI 630A electrochemical analyzer (CH Instruments, Austin, TX) with a bias voltage of +0.1 V.

RESULTS AND DISCUSSION

UV-Irradiation Induced TiO_2 Aggregation. The stability of the TiO_2 nanoparticle suspension was investigated by visual inspection first. As depicted in Figure 1a, the suspension of the pristine nanoparticle was quite stable and did not show any precipitation after 2 h under static state. However, after UV irradiation, the suspension became unstable as some of the particles started to settle at the bottom. After 30 h irradiation, a clear separation between liquid and solid phase in the suspension was seen. TEM examination of the irradiated samples revealed the existence of TiO_2 aggregates. Both the occurrence and size of the aggregates increased appreciably with irradiation duration (Supporting Information (SI) Figure S1). The samples were further characterized by DLS. Average hydrodynamic diameter of the TiO_2 particles before irradiation was found to be approximately 252 nm, consistent with previously reported values.[16] The hydrodynamic size increased progressively as a function of UV irradiation duration, and reached 623 nm after 50 h (Figure 1b). For comparison, the hydrodynamic size of TiO_2 samples without UV irradiation increased only slightly with prolonged agitation time. This indicates that UV irradiation accelerated TiO_2 aggregation.

To investigate aggregation kinetics, the irradiated TiO_2 samples were redispersed by ultrasonication, and the hydrodynamic size went back to the similar level of the unirradiated TiO_2 sample. Then the dispersed TiO_2 sample reaggregated spontaneously, and the aggregation curves were shown in SI Figure S2. Although the hydrodynamic diameter of the pristine nanoparticles did not change during the measurement (6 h), that of the irradiated TiO_2 enlarged substantially. The initial aggregation rate $(((dr_h(t))/(dt))_{t\to 0})$ was determined by linear regression analysis of the aggregation curve. After 50 h of UV irradiation, the aggregation rate increased from an initial value of less than 0.001 to 0.027 nm/s, representing a more than 27 fold increase.

UV Irradiation Induced TiO_2 Transformation. Nanoparticle aggregation is usually considered as a consequence of surface interactions. In order to find the cause for the accelerated TiO_2 nanoparticle aggregation after UV irradiation, some of the surface properties of the TiO_2 particles were investigated. First of all, the zeta potential of the TiO_2 suspension in water was measured in a pH range of 3−10. Based on the pH-dependent profile illustrated in Figure 2a, the isoelectric point (IEP) was determined (SI Table S1). The starting TiO_2 suspension had an IEP of pH 7.00, in agreement with previously reported value for P25 TiO_2.[22] This IEP is much higher than the native pH of the suspension (pH 5.40), indicating that the nanoparticle surface is positively charged, and the suspension is relatively stable due to electrostatic repulsion. Interestingly, the IEP gradually shifted to lower values with prolonged UV irradiation. After 50 h irradiation, the IEP became pH 6.40. In the meantime, the native pH value of the suspension did not change. The lower IEP indicates the particle became less charged, and therefore had higher tendency to aggregate due to the dominance of attractive van der Waals forces over the repulsive electrostatic forces.[23] In Figure 2b, the change of zeta potential with irradiation time measured at pH 5.40 displays the same trend.

dx.doi.org/10.1021/es502360c | Environ. Sci. Technol. 2014, 48, 11962−11968

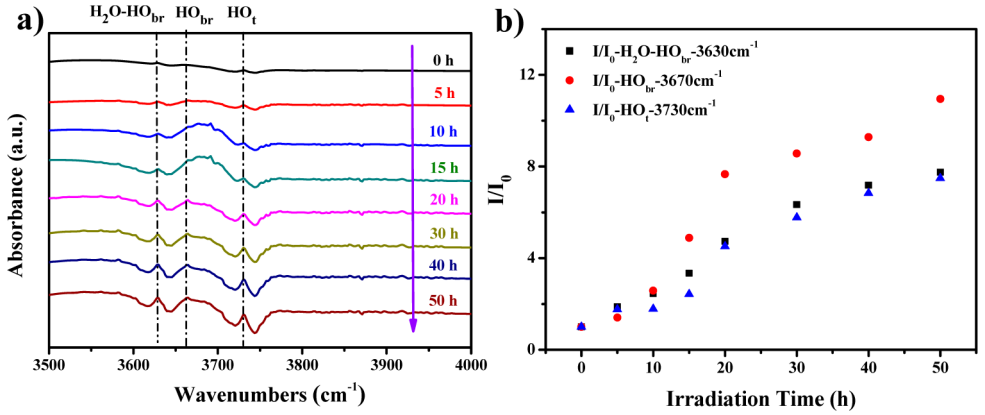

Figure 3. (a) Variation of ATR-FTIR absorption spectra of TiO_2 suspension with UV irradiation time. (b) Variation of the relative peak intensity of stretch mode of bridging hydroxyls (HO_{br}), vibrational mode of terminal hydroxyls (HO_t) and water binding to bridging hydroxyls (H_2O–HO_{br}) in ATR-FTIR spectra as a function of irradiation time. I represents the peak intensity of the hydroxyl band at irradiation time *t*, and I_0 stands for the initial intensity without irradiation.

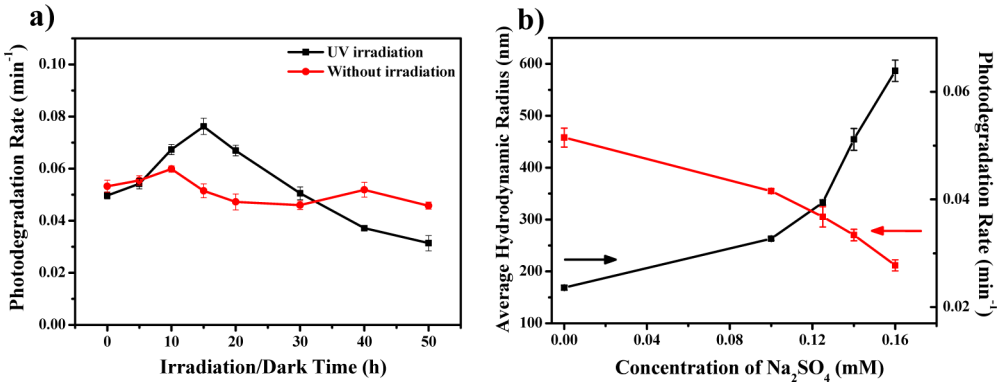

Figure 4. (a) Variation of the photodegradation rate of rohdamine B in TiO_2 suspensions with different UV irradiation time and in nonirradiated TiO_2 suspensions with different stir time; (b) Change of the photodegradation rate and average hydrodynamic diameter of TiO_2 suspension with Na_2SO_4 concentration.

To quantitatively understand the aggregation behavior of the irradiated TiO_2 nanoparticles, the Derjaguin-Landau–Verwey-Overbeek (DLVO) theory was applied to evaluate the van der Waals (VDW) and electrical double-layer (EDL) interactions between the irradiated TiO_2 nanoparticles.[24] The interpretation of the DLVO theory and the calculated nanoparticle–nanoparticle interaction energy are reported in SI (Figure S3). The nanoparticle–nanoparticle interaction energy profiles indicate that energy barriers decrease with the prolonged UV irradiation time. It suggests that UV irradiation favored the nanoparticle–nanoparticle interaction and resulted in the aggregation of nanoparticles. Indeed, the change of the energy barriers is sensitive to the zeta potential of the irradiated TiO_2 nanoparticle based on the primary particle size. Hence, the decreased electrostatic forces may play an important role in controlling the behaviors of TiO_2 nanoparticles. It is important to note that the trends observed in aggregation size are more obvious than the change of the energy barriers, suggesting that DLVO theory cannot fully explain the observed aggregation behavior induced by UV irradiation. This means additional forces, for example, the bridging interactions between acidic bridging hydroxyls and basic terminal hydroxyls on adjacent TiO_2 particles, may also accelerate aggregation process.[25]

The reduction of surface charges after UV irradiation in Figure 2b suggests some structural changes of TiO_2. The crystal structure of the irradiated TiO_2 nanoparticle was evaluated by XRD and Raman spectroscopy. No phase transformation was observed during the irradiation period (SI Figure S4). Surface functional groups of the irradiated nano-TiO_2 were then characterized by in situ ATR-FTIR spectroscopy. With increasing UV irradiation time, the spectra exhibited successive growth of three IR bands centered at 3670, 3730, and 3630 cm^{-1} (Figure 3a), corresponding respectively to the stretch mode of bridging hydroxyls, vibration mode of terminal hydroxyls and water binding to bridging hydroxyls.[25,26] It was reported that, under UV irradiation, the photogenerated holes were trapped at the surface lattice oxygen and created the oxygen vacancies of TiO_2 surface. Subsequently, water molecules dissociated to compensate for these oxygen vacancies and produced surface hydroxyl groups.[27,28] Indeed, most of oxygen vacancies were converted to adsorbed hydroxyl radicals and then released during this process. Quantitative analysis of the three bands revealed a faster formation rate of the bridging hydroxyls than the terminal hydroxyls (Figure 3b). This is because the bridged OH groups have greater thermodynamic stability than terminal OH groups.[29] Since the bridging hydroxyl is acidic (p*K*a 2.9), whereas the terminal hydroxyl is basic (p*K*a 12.7),[30,31] generation of more bridging hydroxyls at pH 5.40 would contribute more negative charges and reduce the overall positive charge on TiO_2 as observed in EPM measurement. This is consistent with the above DLVO calculations. The above results suggest strongly that UV

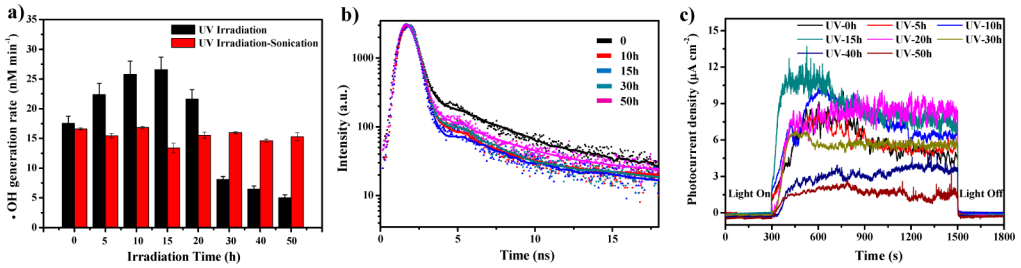

Figure 5. (a) Generation rates of hydroxyl radical of the irradiated TiO_2 suspensions before and after ultrasonic redispersion treatment. (TiO_2: 1 mg L^{-1}, TAOH fluoresces at 426 nm) (b) Photoluminescence decay curves of irradiated TiO_2 aqueous solutions with excitation wavelength at 375 nm and photoluminescence monitored at 430 nm. (c) Time profiles of the photocurrent generation of the irradiated nano-TiO_2 suspensions. Applied potential: + 0.1 V (vs Ag/AgCl electrode).

irradiation of TiO_2 nanoparticles in water preferentially generates bridging hydroxyls on the surface, reduces their surface charge, and consequently promotes particle aggregation.

Impact of Aggregation on TiO_2 Photoreactivity. As a photoactive nanomaterial, nano-TiO_2 has been widely used to catalyze photochemical reactions. However, its photocatalytic properties are closely related to the physicochemical state of the nanoparticles such as the primary particle size as well as the size and structure of nanoparticle aggregates. To evaluate the effect of UV irradiation induced TiO_2 aggregation on its photoreactivity, photocatalytic degradation of RhB by irradiated TiO_2 samples was carried out. In the initial stage of UV irradiation (<15 h), photodegradation rate of RhB increased with irradiation duration. The rate for the 15 h irradiated TiO_2 was 0.075 min^{-1}, up from 0.05 min^{-1}, representing an increase of 50% (Figure 4a). With irradiation longer than 15 h, the degradation rate decreased with the duration and reached 0.03 min^{-1} at 50 h, a 40% drop from its original value. The variation in photocatalytic activity is obviously related to UV irradiation, as the TiO_2 samples without irradiation changed only marginally with time. This result is greatly different from the TiO_2 aggregates induced by inorganic ions. With addition of Na_2SO_4 up to 0.16 mM (without UV irradiation), hydrodynamic size of the TiO_2 aggregates increased from 200 to 600 nm, a size range similar to the UV-irradiated TiO_2 aggregates. However, the photodegradation rate of RhB in Na_2SO_4-induced aggregates decreased monotonically with Na_2SO_4 concentration (Figure 4b). This pattern is substantially different from UV irradiation induced aggregates. The difference in photoreactivity between UV irradiation and salt induced TiO_2 aggregates of similar size suggests the structure of the two aggregates might be different.

Photocatalytic properties of the TiO_2 aggregates were further characterized by hydroxyl radical generation, photoluminescence lifetime and photocurrent measurements. Hydroxyl radical generation rate was quantified by the terephthalic acid (TA) fluorescence assay.[20] As shown in Figure 5a, ·OH generation rate of the TiO_2 samples initially increased with UV irradiation duration up to 15 h, and then decreased with longer irradiation. This trend is the same as the observed photocatalytic degradation rate of RhB. To identify the key factor on the photoreactivity, the irradiated TiO_2 nanoparticles were then redispersed by ultrasonic treatment to investigate their generation of ·OH radicals. Compared with the nonirradiated TiO_2 sample, the ·OH radicals generation of the irradiated and then redispersed TiO_2 samples kept almost unchanged. It needs to note that the aggregation of the redispersed nanoparticles during radical measurements (within 60 min) was almost negligible (SI Figure S2a). Thus, it can be deduced that the aggregate size and structure determine the photoreactivity of the irradiated nano-TiO_2.

In order to explore the impact of aggregation on the charge transfer behavior of the aggregates, transient photoluminescence decay of the TiO_2 suspensions with different irradiation times was measured (Figure 5b). The decay curves were fitted well with a biexponential decay function, with all the fitting parameters listed in SI Table S2. With increasing UV irradiation time up to 15 h, both lifetimes (τ_1 and τ_2) showed a slight decrease, which indicates that TiO_2 particle aggregation facilitated charge separation and charge transfer. However, after 15 h irradiation, the lifetime increased, indicating that the processes were impeded. This result is consistent with the trend of hydroxyl radical generation, since fast charge separation and charge transfer are favorable for radical generation. The charge transfer efficiency of photoexcited TiO_2 was further characterized by photocurrent measurement of UV irradiated TiO_2 suspension, which was conducted in a three-electrode cell under illumination. Once again, the photocurrent gradually increased until 15 h irradiation, and then decreased (Figure 5c and SI Table S3). This indicates that the charge transfer efficiency initially improved with nanoparticle aggregation, and then slowed down.

As described above, the variation of photocatalytic degradation activity of TiO_2 aggregates induced by ionic species showed a monotonic decrease with increasing aggregate size (Figure 4), which is consistent with the results in earlier reports.[16,32] The decrease was mostly attributed to reduced specific surface area and mass diffusion in large aggregates. However, the two-phase variation of the UV irradiation induced TiO_2 aggregates does not correlate with the change of specific surface area. In addition, mass diffusion was not involved in photoluminescence lifetime measurement. Therefore, we need an alternative explanation for the observed pattern of change in their photocatalytic activities. Based on the above photoluminescence lifetime and photocurrent analysis, we hypothesize that, in the absence of electrolytes, there is direct contact between primary TiO_2 nanoparticles in the UV induced aggregates that promotes fast interparticle charge transfer and facilitates charge separation in photoexcited TiO_2. This interparticle charge transfer process in the aggregates has been demonstrated by antenna effect.[33,34] In small aggregates, the separated charges are trapped immediately by the active sites on the outer surface of the aggregate and subsequently participate in the photocatalytic reactions. However, in large aggregates the separated charge carrier may recombine with the opposite charge in another nanoparticle before it reaches the

dx.doi.org/10.1021/es502360c | Environ. Sci. Technol. 2014, 48, 11962−11968

surface. By contrast, in the case of electrolyte-induced TiO_2 aggregates, the particles are surrounded by ions, which would prevent close contact between particles and hinder interparticle charge transfer.[16,35,36]

In summary, UV irradiation of P25 TiO_2 suspension in water was found to increase the surface concentration of hydroxyl groups, particularly bridging hydroxyls in a time-dependent manner. This increase of acidic groups lowered the isoelectric point and reduced the positive charges of TiO_2, leading to enhanced particle aggregation. After 50 h irradiation, the aggregation rate increased to 0.027 nm/s, and hydrodynamic diameter reached 623 nm. TiO_2 aggregation had a significant impact on its photocatalytic activities in a way that is different from ionic species induced aggregation. Our findings on the surface transformation and photocatalytic properties of TiO_2 under UV irradiation would help to better predict the environmental fate and transport of these commonly used nanomaterials, as well as their application performance. Work is currently underway to investigate possible transformation of TiO_2 nanoparticles under UV irradiation in the presence of ions and dissolved organic matters so that the study is more relevant to natural environment.

■ ASSOCIATED CONTENT

Supporting Information

TEM images, aggregation kinetic curves, XRD and Raman spectra, table of pH_{IEP} values, table of biexponential fitting parameters for the photoluminescence decay curve, and total charge of UV-irradiated TiO_2 nanoparticles during illumination time. This material is available free of charge via the Internet at http://pubs.acs.org.

■ AUTHOR INFORMATION

Corresponding Authors

*(L.-H.G.) Phone: 86 10-62849685; e-mail: LHGuo@rcees.ac.cn.

*(H.Z.) Phone: 86 10-62849338; e-mail: huizhang@rcees.ac.cn.

Notes

The authors declare no competing financial interest.

■ ACKNOWLEDGMENTS

This work was supported by the National Basic Research Program of China (2011CB936001, 2010CB933502) and National Nature Science Foundation of China (Nos. 21207146 and 21177138). We are indebted to Prof. Chuanyong Jing, Dr. Shan Hu, Prof. Jingfu Liu, and Dr. Junfang Sun at the Research Centre for Eco-environmental Sciences, Chinese Academy of Sciences for acquiring the ATR-FTIR and Raman spectra.

■ REFERENCES

(1) Hoffmann, M. R.; Martin, S. T.; Choi, W. Y.; Bahnemann, D. W. Environmental applications of semiconductor photocatalysis. *Chem. Rev.* **1995**, *95* (1), 69−96.

(2) Tong, H.; Ouyang, S.; Bi, Y.; Umezawa, N.; Oshikiri, M.; Ye, J. Nano-photocatalytic materials: Possibilities and challenges. *Adv. Mater.* **2012**, *24* (2), 229−251.

(3) Patzke, G. R.; Zhou, Y.; Kontic, R.; Conrad, F. Oxide nanomaterials: Synthetic developments, mechanistic studies, and technological innovations. *Angew. Chem., Int. Ed.* **2011**, *50* (4), 826−859.

(4) Roy, P.; Berger, S.; Schmuki, P. TiO_2 nanotubes: Synthesis and applications. *Angew. Chem., Int. Ed.* **2011**, *50* (13), 2904−2939.

(5) Linsebigler, A. L.; Lu, G. Q.; Yates, J. T. Photocatalysis on TiO_2 surfaces: Principles, mechanisms, and selected results. *Chem. Rev.* **1995**, *95* (3), 735−758.

(6) Legrini, O.; Oliveros, E.; Braun, A. M. Photochemical processes for water-treatment. *Chem. Rev.* **1993**, *93* (2), 671−698.

(7) Robichaud, C. O.; Uyar, A. E.; Darby, M. R.; Zucker, L. G.; Wiesner, M. R. Estimates of upper bounds and trends in nano-TiO_2 production as a basis for exposure assessment. *Environ. Sci. Technol.* **2009**, *43* (12), 4227−4233.

(8) Batley, G. E.; Kirby, J.; Mclaughlin, M. Fate and risks of nanomaterials in aquatic and terrestrial environments. *Acc. Chem. Res.* **2013**, *46* (3), 854−862.

(9) Lowry, G. V.; Gregory, K. B.; Apte, S. C.; Lead, J. R. Transformations of nanomaterials in the environment. *Environ. Sci. Technol.* **2012**, *46* (13), 6893−6899.

(10) Neale, P. A.; Jamting, A. K.; Escher, B. I.; Herrmann, J. A review of the detection, fate and effects of engineered nanomaterials in wastewater treatment plants. *Water Sci. Technol.* **2013**, *68* (7), 1440−1453.

(11) Liu, X. Y.; Chen, G. X.; Keller, A. A.; Su, C. M. Effects of dominant material properties on the stability and transport of TiO_2 nanoparticles and carbon nanotubes in aquatic environments: From synthesis to fate. *Environ. Sci.: Processess Impacts* **2013**, *15* (1), 169−189.

(12) Chowdhury, I.; Cwiertny, D. M.; Walker, S. L. Combined factors influencing the aggregation and deposition of nano-TiO_2 in the presence of humic acid and bacteria. *Environ. Sci. Technol.* **2012**, *46* (13), 6968−6976.

(13) Chowdhury, I.; Walker, S. L.; Mylon, S. E. Aggregate morphology of nano-TiO_2: Role of primary particle size, solution chemistry, and organic matter. *Environ. Sci.: Processes Impacts* **2013**, *15* (1), 275−282.

(14) Hahn, M. W.; Abadzic, D.; O'Melia, C. R. Aquasols: On the role of secondary minima. *Environ. Sci. Technol.* **2004**, *38* (22), 5915−5924.

(15) Hotze, E. M.; Phenrat, T.; Lowry, G. V. Nanoparticle aggregation: Challenges to understanding transport and reactivity in the environment. *J. Environ. Qual.* **2010**, *39* (6), 1909−1924.

(16) Jassby, D.; Farner Budarz, J.; Wiesner, M. Impact of aggregate size and structure on the photocatalytic properties of TiO_2 and ZnO nanoparticles. *Environ. Sci. Technol.* **2012**, *46* (13), 6934−6941.

(17) Pan, L.; Zou, J. J.; Zhang, X.; Wang, L. Water-mediated promotion of dye sensitization of TiO_2 under visible light. *J. Am. Chem. Soc.* **2011**, *133* (26), 10000−10002.

(18) Wang, R.; Hashimoto, K.; Fujishima, A.; Chikuni, M.; Kojima, E.; Kitamura, A.; Shimohigoshi, M.; Watanabe, T. Light-induced amphiphilic surfaces. *Nature* **1997**, *388* (6641), 431−432.

(19) Wang, R.; Hashimoto, K.; Fujishima, A.; Chikuni, M.; Kojima, E.; Kitamura, A.; Shimohigoshi, M.; Watanabe, T. Photogeneration of highly amphiphilic TiO_2 surfaces. *Adv. Mater.* **1998**, *10* (2), 135−138.

(20) Yu, J. G.; Dai, G. P.; Cheng, B. Effect of crystallization methods on morphology and photocatalytic activity of anodized TiO_2 nanotube array films. *J. Phys. Chem. C* **2010**, *114* (45), 19378−19385.

(21) Lakshminarasimhan, N.; Kim, W.; Choi, W. Effect of the agglomerated state on the photocatalytic hydrogen production with in situ agglomeration of colloidal TiO_2 nanoparticles. *J. Phys. Chem. C* **2008**, *112* (51), 20451−20457.

(22) Gumy, D.; Morais, C.; Bowen, P.; Pulgarin, C.; Giraldo, S.; Hajdu, R.; Kiwi, J. Catalytic activity of commercial of TiO_2 powders for the abatement of the bacteria (*E. coli*) under solar simulated light: Influence of the isoelectric point. *Appl. Catal., B* **2006**, *63* (1−2), 76−84.

(23) Derjaguin, B.; Landau, L. Theory of the stability of strongly charged lyophobic sols and of the adhesion of strongly charged-particles in solutions of electrolytes. *Prog. Surf. Sci.* **1993**, *43* (1−4), 30−59.

(24) Chen, G.; Liu, X.; Su, C. Transport and retention of TiO_2 rutile nanoparticles in saturated porous media under low-ionic-strength

conditions: Measurements and mechanisms. *Langmuir* **2011**, *27* (9), 5393−5402.
(25) Soria, J.; Sanz, J.; Sobrados, I.; Coronado, J. M.; Hernandez-Alonso, M. D.; Fresno, F. Water-hydroxyl interactions on small anatase nanoparticles prepared by the hydrothermal route. *J. Phys. Chem. C* **2010**, *114* (39), 16534−16540.
(26) Finnie, K. S.; Cassidy, D. J.; Bartlett, J. R.; Woolfrey, J. L. IR spectroscopy of surface water and hydroxyl species on nanocrystalline TiO_2 films. *Langmuir* **2001**, *17* (3), 816−820.
(27) Sakai, N.; Fujishima, A.; Watanabe, T.; Hashimoto, K. Quantitative evaluation of the photoinduced hydrophilic conversion properties of TiO_2 thin film surfaces by the reciprocal of contact angle. *J. Phys. Chem. B* **2003**, *107* (4), 1028−1035.
(28) Zhang, J.; Nosaka, Y. Mechanism of the OH radical generation in photocatalysis with TiO_2 of different crystalline types. *J. Phys. Chem. C* **2014**, *118* (20), 10824−10832.
(29) Murakami, Y.; Endo, K.; Ohta, I.; Nosaka, A. Y.; Nosaka, Y. Can OH radicals diffuse from the UV-irradiated photocatalytic TiO_2 surfaces? Laser-induced-fluorescence study. *J. Phys. Chem. C* **2007**, *111* (30), 11339−11346.
(30) Boehm, H. P. Acidic and basic properties of hydroxylated metal-oxide surfaces. *Discuss. Faraday. Soc.* **1971**, *52*, 264−227.
(31) Tran, T. H.; Nosaka, A. Y.; Nosaka, Y. Adsorption and photocatalytic decomposition of amino acids in TiO_2 photocatalytic systems. *J. Phys. Chem. B* **2006**, *110* (50), 25525−25531.
(32) Folli, A.; Pochard, I.; Nonat, A.; Jakobsen, U. H.; Shepherd, A. M.; Macphee, D. E. Engineering photocatalytic cements: Understanding TiO_2 surface chemistry to control and modulate photocatalytic performances. *J. Am. Ceram. Soc.* **2010**, *93* (10), 3360−3369.
(33) Lakshminarasimhan, N.; BokarE, A. D.; Choi, W. Effect of agglomerated state in mesoporous TiO_2 on the morphology of photodeposited Pt and photocatalytic activity. *J. Phys. Chem. C* **2012**, *116* (33), 17531−17539.
(34) Wang, C. Y.; BÖttcher, C.; Bahnemann, D. W.; Dohrmann, J. r. K. A comparative study of nanometer sized Fe(iii)-doped TiO_2 photocatalysts: Synthesis, characterization and activity. *J. Mater. Chem.* **2003**, *13* (9), 2322−2329.
(35) Rachel, A.; Subrahmanyam, M.; Boule, P. Comparison of photocatalytic efficiencies of TiO_2 in suspended and immobilised form for the photocatalytic degradation of nitrobenzenesulfonic acids. *Appl. Catal., B* **2002**, *37* (4), 301−308.
(36) Guillard, C.; Puzenat, E.; Lachheb, H.; Houas, A.; Herrmann, J. M. Why inorganic salts decrease the TiO_2 photocatalytic efficiency. *Int. J. Photoenergy* **2005**, *7* (1), 1−9.
(37) Petosa, A. R.; Jaisi, D. P.; Quevedo, I. R.; Elimelech, M.; Tufenkji, N. Aggregation and deposition of engineered nanomaterials in aquatic environments: Role of physicochemical interactions. *Environ. Sci. Technol.* **2010**, *44* (17), 6532−6549.